Bone 125 (2019) 36–45

Contents lists available at ScienceDirect

Bone

journal homepage: www.elsevier.com/locate/bone

Full Length Article

Subject-specific *ex vivo* simulations for hip fracture risk assessment in sideways falls

Ingmar Fleps[a,c,*], Anita Fung[a,c], Pierre Guy[b], Stephen J. Ferguson[a], Benedikt Helgason[a], Peter A. Cripton[c]

[a] Institute for Biomechanics, ETH Zürich, Zürich, Switzerland
[b] Division of Orthopaedic Trauma, Department of Orthopaedics, University of British Columbia, Vancouver, Canada
[c] Orthopaedics and Injury Biomechanics Group, Departments of Mechanical Engineering and Orthopaedics and School of Biomedical Engineering, University of British Columbia, Vancouver, Canada

A B S T R A C T

The risk of hip fracture of a patient due to a fall can be described from a mechanical perspective as the capacity of the femur to withstand the force that it experiences in the event of a fall. So far, impact forces acting on the lateral aspect of the pelvic region and femur strength have been investigated separately. This study used inertia-driven cadaveric impact experiments that mimic falls to the side from standing in order to evaluate the subject-specific force applied to the hip during impact and the fracture outcome in the same experimental model. Eleven fresh-frozen pelvis-femur constructs (6 female, 5 male, age = 77 years (SD = 13 years), BMI = 22.8 kg/m^2 (SD = 7.8 kg/m^2), total hip aBMD = 0.734 g/cm^2 (SD = 0.149 g/cm^2)), were embedded into soft tissue surrogate material that matched subject-specific mass and body shape. The specimens were attached to metallic lower-limb constructions with subject-specific masses and subjected to an inverted pendulum motion. Impact forces were recorded with a 6-axis force plate at 10,000 Hz and three dimensional deflections in the pelvic region were tracked with two high-speed cameras at 5000 Hz. Of the 11 specimens, 5 femur fractures and 3 pelvis fractures were observed. Three specimens did not fracture. aBMD alone did not reliably separate femur fractures from non-fractures. However, a mechanical risk ratio, which was calculated as the impact force divided by aBMD, classified specimens reliably into femur fractures and non-fractures. Single degree of freedom models, based on specimen kinetics, were able to predict subject-specific peak impact forces (RMSE = 2.55% for non-fractures). This study provides direct evidence relating subject-specific impact forces and subject-specific strength estimates and improves the assessment of the mechanical risk of hip fracture for a specific femur/pelvis combination in a sideways fall.

1. Introduction

Hip fracture poses a serious health threat to the elderly. It is considered the most devastating of osteoporotic fractures with severe consequences on morbidity, mental health, and an increased risk of mortality [1–3]. In the European Union alone, 610,000 new hip fractures were registered in 2010 and are expected to reach 810,000 fractures per year by 2025. By then, the direct medical cost associated with this type of fracture will be 25.3 billion euros per year [4]. Epidemiological evidence suggests that the majority of hip fractures are the result of a fall from standing or lower height with subsequent impact on the greater trochanter (GT) [5]. While falls in the elderly are frequent [6,7], only about 1–5% of falls result in a fracture [8–10]. Therefore, one might wonder what sets these patients or falls apart from others that do not lead to fracture. Current clinical diagnostic tools, derived from dual energy X-ray absorptiometry (DXA), rely on areal bone mineral density (aBMD) measurements to evaluate bone fragility and the subsequent risk of fracture. Other tools like the Fracture Risk Assessment Tool (FRAX) also consider lifestyle factors and patient anthropometry. Unfortunately, both of these tools have demonstrated limited sensitivity in terms of identifying patients at risk [11–15]. Bone strength derived with image-based finite element analysis (FEA) was demonstrated to be superior to aBMD in terms of the prediction of *ex-vivo* measured femoral strength in a sideways fall loading configuration [16–19]. However, when these models have been generated from image data acquired at baseline and used to quantify hip fracture risk in clinical cohorts over a given follow-up period, these models have provided no improvement beyond aBMD [20–27]. Only when these models were generated based on image data gathered post-fracture did these models demonstrated significantly higher AUC derived from receiver operator characteristic analysis [28–30]. The models in these studies either neglected the effect of patient-specific impact force that is transferred to the femur as the result of a fall, or predicted the impact force with simplified analytical models. A recent study that uses patient-specific single degree of freedom spring mass models (sDOF models) demonstrated that patient-specific impact loads may influence the hip fracture risk [31]. Input information for these type of models is difficult to obtain because controlled fall experiments with volunteers are challenging and limited

* Corresponding author at: Institute for Biomechanics, ETH Zürich, Zürich, Switzerland.
E-mail address: Ingmar.fleps@hest.ethz.ch (I. Fleps).

https://doi.org/10.1016/j.bone.2019.05.004
Received 21 December 2018; Received in revised form 17 April 2019; Accepted 4 May 2019
Available online 06 May 2019
8756-3282/

to low-energy impacts that do not pose any risk of fracture [32,33]. Another approach entails working with human volunteers and simulating falls onto soft protective surfaces that reduce the force acting on the volunteers [31,34]. To predict forces at impact conditions representative of a fall from standing, these models rely on extrapolation far beyond the force range for which they were validated [25,31,33,35,36]. *Ex vivo* models using post-mortem human tissue allow for testing of human femurs up to injurious load levels. However, state-of-the-art impact models that have modelled a fall to the side either did not consider the compliant structures (overlying soft tissue and the compliant pelvis) around the femur [19] or considered surrogate models for the pelvis and soft tissues, but did not model patient-specific impact loads [37]. Other cadaveric side-impact models, which considered full pelvis-femur constructs, used impact boundary conditions that were representative of vehicle side impact collisions rather than sideways falls, and generated pelvic fractures but no femoral fractures [38–41]. All of these cadaveric studies impacted rigid masses onto stationary specimens as opposed to dropping the specimen from height with an impact at the greater trochanter, which is more representative of a person falling.

In the present study we used our recently-published cadaveric inverted pendulum protocol to simulate sideways falls [42]. This protocol models the lower extremities of the human body up to the navel according to subject-specific anthropometrics. We used this protocol to systematically investigate the mechanical response of the human body undergoing impact to the hip due to a fall. The protocol focuses on the influence of impact energy, soft tissue mass and geometry, pelvic compliance, and bone mineral density on the mechanical response of the pelvic region. We hypothesised that due to the non-linearity of the system's force-displacement response and the limited soft tissue deformation over the greater trochanter, the effective pelvic stiffness derived from these experiments would be considerably higher than effective pelvic stiffness values derived from less severe loading conditions with volunteers. Secondly, we hypothesised that subject-specific impact simulations representative of a fall from standing would result in femur fractures and non-fracture outcomes that cannot be explained by bone mineral density alone. Finally, we hypothesised that a mechanical hip fracture risk assessment which includes both the impact force and aBMD would be superior to hip fracture risk assessment based on aBMD alone.

2. Materials and methods

2.1. Experimental testing

This study was approved by the University of British Columbia Clinical Research Ethics Board (Study ID H06-70337). Experiments and specimen preparation were carried out at two UBC research centres: The centre for Hip Health and Mobility and the International Collaboration On Repair Discoveries (ICORD). Specimen preparation and experiments were conducted according to the protocol published in Fleps et al. [42]. In short, 11 fresh-frozen post-mortem human specimens including all tissues between the navel and mid-femur were acquired from a tissue bank (ScienceCare, Phoenix, AZ, USA) (Table 1).

Table 1
Specimen information.

$N = 11$	Unit	Average (STD)	Range
Age	[years]	77.1 (13.4)	54–94
Height	[m]	1.69 (0.08)	1.56–1.82
Body mass	[kg]	64.3 (18.4)	40.8–99.8
BMI	[kg/m^2]	22.7 (7.8)	14.8–40.2
$T_{ST,GT}$	[mm]	26 (21)	7–73
Total hip aBMD	[g/cm^2]	0.735 (0.149)	0.559–1.129
T-score	[ ]	−1.6 (1.3)	−3.1–1.8

Donors or a next to kin had given written or electronic consent to the donation.

The pelvis-femur constructs were dissected. Muscles were meticulously stripped while bone, cartilage, joint capsules, and ligaments were kept intact. Mechanical connectors were attached to the distal femurs and the base of sacrum. The specimens were embedded in 20 wt% ballistic gelatin to simulate soft tissues with subject-specific shapes and masses in a controlled manner. The mechanical properties of the ballistic gelatin lay within the properties of muscle and adipose tissue tested in compression [43–45]. The soft tissue contours were matched from a surface scan database (SizeUSA, [TC]^2 Labs, Apex, NY, USA) using body mass, body height, the maximum distance between both greater trochanters, and the target soft tissue thickness over the greater trochanter ($T_{ST,GT}$). $T_{ST,GT}$ was calculated as a function of BMI [46,47]. The embedded specimens were attached to metallic lower limb constructions comprising the lower femur, knee angle, entire tibia, and ankle. The surrogate lower extremities were weighted to subject-specific masses, but leg length and alignment angles remained fixed such that a greater trochanter height of 0.76 m in a flexed leg position resulted (Fig. 1). The alignment of the impacted femur was controlled so the femur would impact with the neck axis aligned in a vertical plane. Details on specimen alignment are reported in the study that describes the protocol [42].

Specimens were guided with rollers attached to each leg and the pelvis to constrain the fall motion to an inertia-driven single degree of freedom inverted pendulum motion. Our study focuses on the influence of subject anthropometric on the impact kinetics, therefore all specimens were released from the same height and with the same greater trochanter height to create impacts with a reproducible impact velocity. Constraints were released prior to impact as the rollers slipped of cut guidance surfaces. Only the translational constraints of the ipsilateral foot point were maintained, creating a minimally constrained impact at the hip that allowed for ipsilateral leg rotation, pelvic rotation, and contralateral leg motion.

Clinical resolution quantitative computed tomography scans (qCT) were obtained for each specimen (120 kVp, 200 mAs, voxel size: 0.78 mm × 0.78 mm × 0.3 mm) before it was embedded in the soft tissue surrogate material that represented muscle, skin, and adipose tissue. A hydroxyapatite calibration phantom (QC1, Scanco Medical, Brüttisellen, Switzerland) was scanned with each specimen for linking greyscale values to bone density. QCT base aBMD measurements were obtained using a commercial tool (QCT Pro, Mindways Software, Inc., Austin, Texas). QCT based aBMD values have been shown to be highly correlated to DXA based aBMD measurements [48,49].

2.2. Data collection

The force at the impact surface was measured with a modified six-axis force plate (FP4000–15, Bertec Corporation, Columbus, OH, USA), collecting at a sampling rate of 10,000 Hz. A total of 14 spherical markers (CTMark (4 mm), Suremark®, Simi Valley, CA, USA) placed on the surface of the pelvis and soft tissue surrogate (Fig. 1) were tracked in 3D at a frame rate of 5000 Hz with a stereo camera system (Phantom v12, Vision Research, Wayne, NJ, USA). Marker tracking had an accuracy of 0.07 mm, 0.08 mm, and 0.44 mm in the global x, y and z directions, respectively. A third high-speed camera (Phantom v9, Vision Research, frame rate 200 Hz) and a digital camera (frame rate of 50 Hz) were used to capture the overall pendulum motion and impact. Direct linear transformation [50] with a static calibration cage was used to reconstruct 3D coordinates. Two active infrared-emitting markers with a sampling frequency of 300 Hz, fixed to the impacted leg, were used to track the impacted leg over time. The impact velocity (v_{imp}) was determined by calculating a rigid body motion using the two active markers and the translationally fixed foot point. The impact velocity was defined as the velocity at the time of first contact of the specimen with the impact surface ($F > 20$ N). Two-dimensional X-ray images

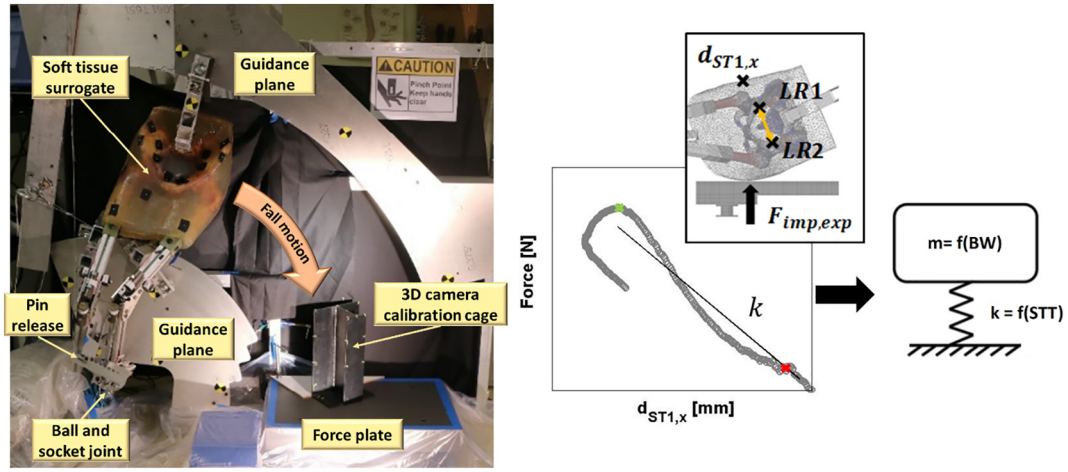

Fig. 1. Inverted pendulum setup with specimen H1401 ready for testing. The image in the top right shows the marker that was used for the evaluation of the effective pelvic stiffness. The graph indicates the linear regression that was calculated in the range from 500 N to peak force, which are indicated with a red and a green cross, respectively. (For interpretation of the references to colour in this figure legend, the reader is referred to the web version of this article.)

were taken with a mobile X-ray unit (Mobile 100-15, General Electrics, Boston, MA, USA) prior and post testing for fracture evaluation.

2.3. Data analysis

Fracture outcome was assessed by an orthopaedic surgeon (PG) based on planar radiographs and specimen dissections after testing. The soft tissue thickness over the greater trochanter was measured based on digitized surface points of the soft tissue and femur after embedding the specimens in the soft tissue surrogate. This measurement was verified by measuring the thickness of the soft tissue over the greater trochanter with a ruler during dissection of the soft tissue surrogate material after testing. The time from first contact with the force plate to peak load ($t_{F_{peak}}$) was derived from the impact response. The angular momentum (p_{rot}) for each impact was calculated as the product of the mass moment of inertia around the rotation axis (I_Z) and the rotational velocity (ω) of the pendulum at first contact of the specimen with the force plate (eq. 1). The rotational mass moment of inertia was determined based on detailed CAD models of each specimen. The torque impulse (T) up to peak force was calculated by integrating the impulse response and multiplying it with the distance from the centre of rotation at the foot point to the centre of pressure on the force plate (r_{GT}) (Eq. (2)).

$$p_{rot} = I_Z \bullet \omega \tag{1}$$

$$T = \int_{t=t_0}^{t_{F_{peak}}} F(t) \bullet dt \bullet r_{GT} \tag{2}$$

The pelvic compression (C_{LR}) was evaluated by tracking the change in distance between marker pair LR1 and LR2 (Fig. 1). Maximum pelvic compression $C_{LR,max}$ and pelvic compression at 80% of peak force $C_{LR}(F_{80\%})$ were quantified.

In order to compare to existing impact models for simulating sideways falls loading, we calculated the effective pelvic stiffness of the pelvic region based on the impact force as a function of the contralateral soft tissue deflection. This force-deflection response was reported to be non-linear for impact experiments with volunteers [32,51]. However, single degree of freedom (sDOF) models with a linear spring stiffness showed lower errors in predicted peak forces when compared to impact experiments with volunteers than models that used a non-linear spring stiffness [32]. Furthermore, our recent computational study indicated that large amounts of the initial kinetic energy remains kinetic energy at the time of peak force, which is not captured by a sDOF model comprised of a spring and mass only. Lacking the information for a more complex spring-mass model, which might capture the non-linear force deflection characteristic and the energy balance in the system, we derived a linear effective stiffness values (k) for comparison to existing literature. k was calculated by fitting a linear regression model to the impact force as a function of the contralateral soft tissue marker motion perpendicular to the impact surface ($d_{ST1,x}$), in the force interval from 500 N to peak force. This method is analogue to the effective pelvic stiffness determined from low drop height experiments with volunteers [32]. These models will hereafter be referred to as **model 1** (k_{m1}). The interval from 500 N to peak force was selected to avoid bias due to inertial effects at first contact with the impact surface.

A second model, hereafter referred to as **model 2** (k_{m2}), modelled the effective pelvic stiffness as a function of $T_{GT,ST}$. This dependency was determined with linear regression between the inverse of the effective pelvic stiffness ($1/k_{m1}$) and $T_{GT,ST}$. No damping was considered for models 1 and 2.

For comparison with existing impact models, sDOF models from literature were implemented that used input information from testing with volunteers at less severe conditions. Based on data presented in Robinovitch et al. [33] an effective pelvic stiffness (k) and damping (b) as a function of soft tissue thickness were calculated and implemented. Based on Laing et al. [32], a single effective stiffness was implemented. For Sarvi et al. [52], a linear fit for k and b with BMI was calculated

Table 2
sDOF parameters [31–33,52].

Study	k [N/mm]	Range k [N/mm]	b [Ns/m]	Range b [Ns/m]
Robinovitch et al. (1991)	$\frac{1}{k} = 0.00759 + T_{GT,ST} \bullet 0.00085$	13.9–73.9	340	340
Laing et al. (2010) (k1st)	20.9	20.9	0	0
Sarvi et al., 2014	$k = 6.86 \cdot BMI - 75$	26.5–200.8	$b = 87.1 \cdot BMI - 1306$	0–2195.4
Luo et al. (2014)	$k = -7.9 \cdot BMI + 270$	0–153.1	$b = 47 \cdot BMI - 460$	235.6–1429.4
Present study (model 1)	k_{m1}	58.5–483.9	0	0
Present study (model 2)	k_{m2} ($T_{GT,ST}$)	54.1–371.3	0	0

based on their published values. These relationships were then used to calculate k and b values for the specimens tested in our study.

For Luo et al. [31], the published relationship between k and BMI and b and BMI was implemented (Table 2). The effective mass for each specimen was calculated for the translational sDOF model to match the rotational energy of the *ex vivo* experiment (Eq. (3)).

$$m_{eff} = \frac{I_Z}{{r_{gt}}^2} \tag{3}$$

r_{gt} is the distance from the rotational centre at the foot point to the impact point at the greater trochanter. The impact velocity of the greater trochanter was used for the sDOF model. The differential equation of motion (Eq. (4)) was then solved considering the gravitational force (F_G), calculated as the product of the gravitational constant (g) times the effective mass, as an external force. An initial displacement $x_0 = 0$ and an initial velocity $\dot{x}_0 = v_{imp}$, that was derived from the experimental data, were imposed onto the system. The velocity v_{imp} is the product of the angular velocity of the pendulum setup and the distance from the rotational point at the foot to the greater trochanter impact point. The maximum force (F_{peak}) acting onto the mass was then calculated as the maximum of the combination of spring force and dashpot force (Eq. (5)).

$$m\,\ddot{x} + b\,\dot{x} + k\,x = m \bullet g = F_G \tag{4}$$

$$F_{peak} = \max(b\,\dot{x} + k\,x) \tag{5}$$

$F_{peak,m2}$, calculated with model 2, was used to predict the impact force that each specimen would have had to sustain in order not to fracture. aBMD, which is found to be highly correlated with femoral strength in cadaver studies [53–55], was used as a surrogate measure of femoral strength. The mechanical risk ratio (MRR, Eq. (6)), which is the ratio between $F_{peak,m2}$ and aBMD, was used as a predictor of the mechanical risk of fracture.

$$\textit{Mechanical risk ratio (MRR)} = \frac{F_{peak,m2}\ [in\ kN]}{\textit{total hip aBMD}\ \left[in \frac{g}{cm^2}\right]} \tag{6}$$

Similar ratios had been proposed for the evaluation of fracture risk [56], however no experimental data was available to test the potential of these metrics.

3. Results

Of the 11 specimens that were tested, five fractured the proximal femur, four fractured the pubic ramus close to the pubic symphysis and the ischial ramus, and three specimen did not fracture (Fig. 2). Specimen H1389 fractured first the femur and then the pelvis. According to AO classification, the femur fractures were two neck fractures, one subcapital and one basi-cervical, and three intertrochanteric fractures. Four pelvic fractures were observed, all of which were shear fractures at the pubic ramus close to the pubic symphysis. The ischial ramus on the same side was also damaged but did not fail catastrophically.

3.1. Impulse response

Specimens impacted the force plate with a reproducible greater trochanter velocity of 3.07 m/s (SD = 0.06 m/s). Peak impact forces between 2947 N and 7601 N were recorded. For one male specimen (H1401) the force was not recorded due to an operator error. A non-linear impulse response up to peak force was observed for all specimens (Fig. 3). Specimens that fractured the femur had a characteristic sharp drop in peak force right after fracture, followed by a second loading peak. Specimens that fractured the pelvis demonstrated less spontaneous unloading and did not exhibit a secondary loading peak. The time to peak force was strongly correlated with soft tissue thickness over the greater trochanter ($R^2 = 0.963$, Fig. 4 left). A strong correlation was also found between the time to peak force and the fraction of angular momentum that was represented by the torque impulse to peak force ($R^2 = 0.891$, Fig. 4 right).

Male specimens had a higher pelvic stiffness compared to female specimens at 80% peak force (Fig. 5) (non-parametric Mann–Whitney Test, $p = 0.38$). Corresponding results were found for C_{LR} at peak force and the maximum lateral ring compression ($C_{LR,max}$). Table 3 summarized the fall outcomes and the obtained metrics for the *ex vivo* experiments.

3.2. sDOF-based force prediction

The characteristic of the force over contralateral soft tissue marker deflection ($d_{ST1,x}$) in the X direction was non-linear (Fig. 6) and dependent on specimen anthropometrics. Qualitatively, a stronger non-linearity was observed for specimens with thinner trochanteric soft tissue thickness compared to specimens with thicker trochanteric soft tissue thickness. Larger deflections were measured for specimens with thicker greater trochanter soft tissue compared to specimens with thinner trochanteric soft tissue. (Fig. 6, left) The calculated effective pelvic stiffness (k_{m1}) ranged between 58.5 N/mm to 483.9 N/mm and decreased with soft tissue thickness (Fig. 7). The inverse of the effective pelvic stiffness ($1/k_{m1}$) and the greater trochanter soft tissue thickness were highly correlated ($R^2 = 0.94$). The resulting linear regression model was used to calculated k_{m2}. The effective mass was calculated to be 38.1% (SD 2.1%) of body weight. For specimens that did not fracture (H1391, H1395, H1402), a good agreement between the experimental measured peak forces and the peak force predicted by the sDOF models was found. The root mean square errors (RMSE) for these 3 specimens were 3.9% and 6.8% for model 1 and model 2, respectively. For specimens that experienced a fracture, similar peak forces or over predictions were observed (Fig. 8). Literature-based models underestimated the peak force for the non-fracture specimens (Fig. 7) and frequently predicted lower forces than the experimentally measured forces for specimens that fractured (Fig. 8). Details on sDOF model implementations and impact kinetics can be found in the supplementary material.

Peak forces predicted by model 1 and sDOF models based on Robinovitch et al. were strongly correlated but statistically significantly different in magnitide ($R^2 = 0.88$, $p < 0.001$). Weak correlation and statistically significant differences were found for peak forces predicted by model 1 and sDOF models based on Laing et al. ($R^2 = 0.06$, $p < 0.001$), Sarvi et al. ($R^2 = 0.19$, $p = 0.018$), and Luo et al. ($R^2 = 0.18$, $p = 0.002$). Peak forces between model 1 and model 2 were highly correlated and not statistically significantly different ($R^2 = 0.91$, $p = 0.374$). Details on the implemented sDOF models, force-time characteristics and force-displacement characteristics are provided in supplementary material (S2_sDOF_models).

No threshold for total hip aBMD, trochanteric aBMD, and femoral neck aBMD alone could be found which would allow for a separation of femur fractures from non-fracture outcomes (Fig. 9 left). Impact energy was a poor predictor of peak force and fracture outcome. Greater trochanter soft tissue thickness alone was also not predictive of fracture outcome. The mechanical risk ratio (MRR) separated femur fractures and non-fractures reliably (Fig. 9, right). Separations were also observed for alternative MRRs that were calculated with femoral neck aBMD and trochanteric aBMD, as well as when using k_{m1} for the sDOF models. No clear separation for pelvic fractures was observed. MRRs calculated based on peak forces predicted with the effective pelvic stiffness that was derived from Robinovitch et al. also separated femur fractures from non-fractures, but resulted in much lower values due much lower predicted peak force values.

4. Discussion

The goal of this study was to investigate the kinetics of subject-

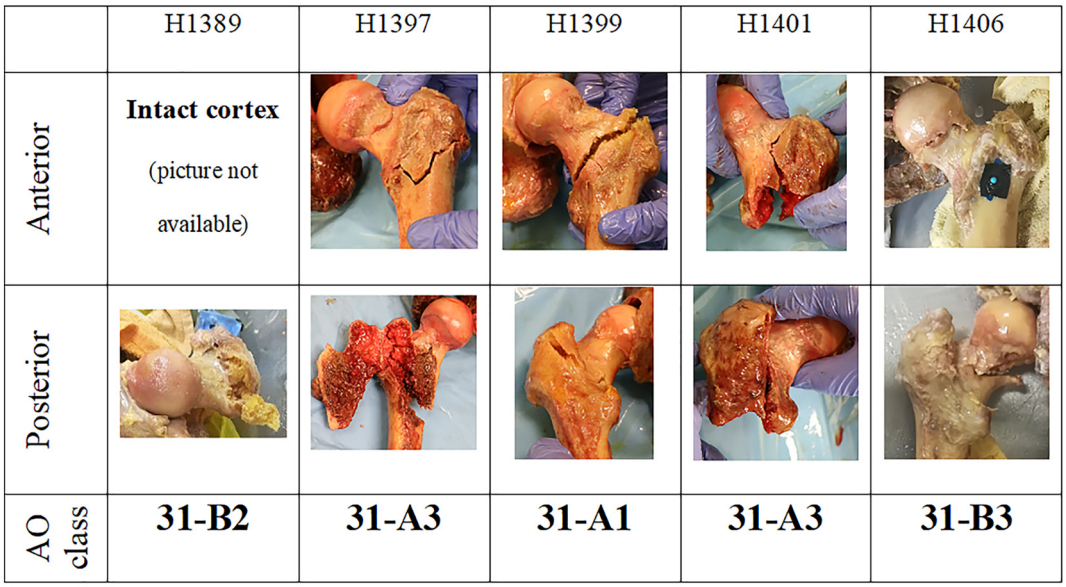

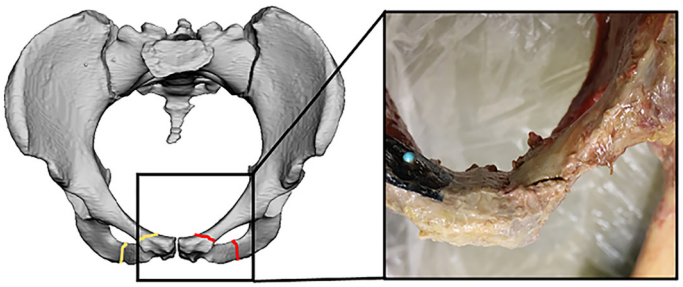

Fig. 2. Fracture outcomes for all 5 femoral fractures (top) and a schematic illustration of the observed pelvic fractures with a close up of specimen H1392 (bottom). Specimen H1394 fractured the contralateral superior and inferior ramus (marked in yellow). (For interpretation of the references to colour in this figure legend, the reader is referred to the web version of this article.)

specific impacts that are representative of a fall to the side from standing height. We hypothesised that impacts up to higher force magnitudes will result in higher effective pelvic stiffness values and found them to be 2–5 times higher in our study compared to effective pelvic stiffness values that were reported based on less severe impact conditions [31–33,52]. Furthermore, we hypothesised that, using this protocol, we would observe both femur fractures and non-fracture outcomes and found this to be the case. However, we also observed pelvis fractures, which are a common fall-related injury in the elderly and are thus clinically relevant and part of the spectrum of injuries we should have expected [13,57,58]. Finally, we hypothesised that, when simulating subject-specific falls, a metric that considers the impact force and aBMD would be superior at predicting femur fractures and non-fracture outcomes compared to aBMD alone. The MRR separated the 5 femur fractures from the 3 non-fracture outcomes, while aBMD alone was unable to separate femur fracture from non-fracture outcomes. This demonstrates how incorporating accurate impact force predictions could improve screening for hip fracture risk.

The force-displacement response of the system under impact was non-linear. Moreover, the kinetics showed a strong dependency on the thickness of soft tissue over the impacted greater trochanter. This is reflected in clinical studies, which report that low BMI, which is

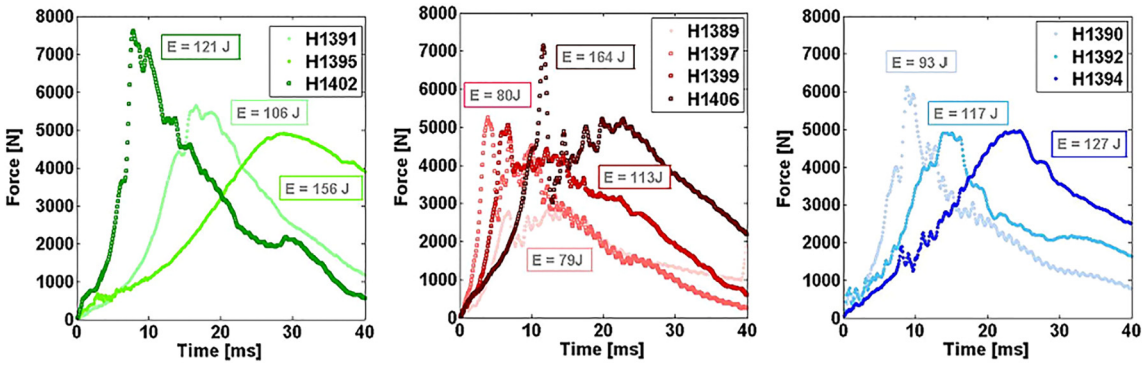

Fig. 3. Impulse response for non-fractures (left), femoral fractures (middle) and pelvic fractures (right).

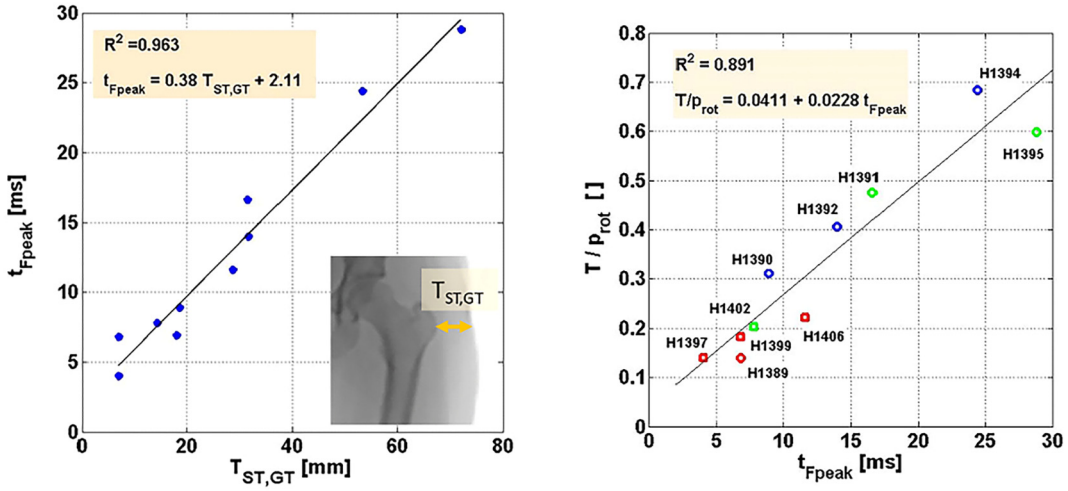

Fig. 4. (left) Relationship between time to peak force and greater trochanter soft tissue thickness and (right) the fraction of initial angular momentum that is represented in the measured torque impulse over time to peak force. Fracture outcomes are indicated by colours: femur fractures (red), pelvis fractures (blue), no fracture (green). (For interpretation of the references to colour in this figure legend, the reader is referred to the web version of this article.)

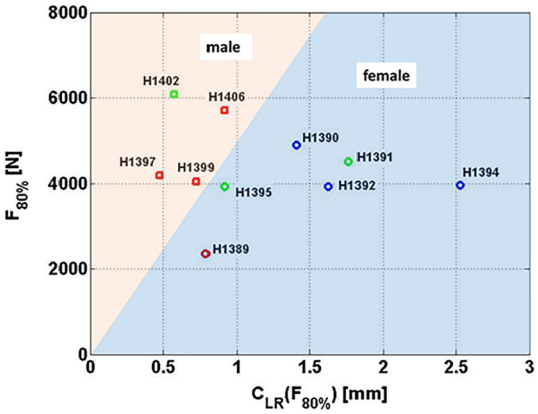

Fig. 5. 80% peak force *versus* lateral ring compression of the pelvis at 80% peak force ($C_{LR}(F_{80\%})$). Fracture outcomes are indicated by colours: femur fractures (red), pelvis fractures (blue), no fracture (green). (For interpretation of the references to colour in this figure legend, the reader is referred to the web version of this article.)

correlated with low trochanteric soft tissue thickness, is a factor for increased fracture risk [59,60]. 94% of the variation in the effective pelvic stiffness derived from the experiments was explained by trochanteric soft tissue thickness, underlining the high importance of soft tissue compared to the stiffness of harder tissues like the femur or the pelvis.

The observed femur and pelvis fractures are comparable to fractures that have been observed clinically as the result of a fall [57,61–64]. The mixture of fracture and non-fracture outcomes allows for direct validation of metrics that can be used for fracture risk assessment. Furthermore, the experiment demonstrates that, even under severe impact conditions, some subjects might not fracture their femur. Together with different fall scenarios, these experiments might help to explain why only 1–5% of falls result in fractures even though the energy absorption of the femur (< 20 J) is much lower than the energy related to typical falls (62–169 J in this study) [8,17,37,65,66]. The high prevalence of pelvis fractures in female specimens over pelvis fractures in male specimens is representative of the clinical incidence. Epidemiological studies reported about 5 times more pelvic fractures in women than in men [13,57,58]. However, the high ratio of femur fractures in male specimens to femur fractures in female specimens is atypical. Epidemiological studies report an about three times higher incidence of femoral fractures in women than in men [2,13], which might be due to a combination of low specimen number, fall alignment, and absence of muscle activation in our model. Compared to other published impact models, our *ex vivo* experiments are the first to generate femur fractures, pelvis fractures, and non-fracture outcomes as the result of simulated sideways fall. Previous sideways fall impact models incorporating the pelvis had failed to create femoral fractures and did not use subject-specific impact conditions [38–40]. Studies that resulted in femoral fractures [19,37] used generic impact conditions for all specimens and did not produce any non-injurious impacts. All of these impact simulations used inverted boundary conditions with a stationary

Table 3
Summary of experimental results.

	F_{max}	t_{Fpeak}	C_{LR},max	C_{LR}(F80%)	k_{m1}	m_{eff}	Fracture type
	[N]	[ms]	[mm]	[mm]	[N/mm]	[kg]	
H1389	2947	6.8	17.8	0.8	199.8	16.8	Femoral neck (basi-cervical) and ipsilateral rami
H1390	6131	8.9	13.0	1.4	163.9	19.0	Ipsilateral rami
H1391	5641	16.6	2.5	1.8	134.7	22.3	–
H1392	4907	14	17.0	1.6	91.9	23.9	Ipsilateral rami
H1394	4958	24.4	16.6	2.5	136.8	28.7	Contralateral rami
H1395	4910	28.8	1.7	0.9	58.5	35.2	–
H1397	5242	4	0.8	0.5	483.9	18.1	Intertrochanteric
H1399	5043	6.8	1.8	0.7	405.8	24.2	Intertrochanteric
H1401	–	–	4.1	–	–	19.8	Intertrochanteric
H1402	7601	7.8	1.0	0.6	210.0	25.1	–
H1406	7132	11.6	1.2	0.9	143.0	34.1	Femoral neck (sub-capital)

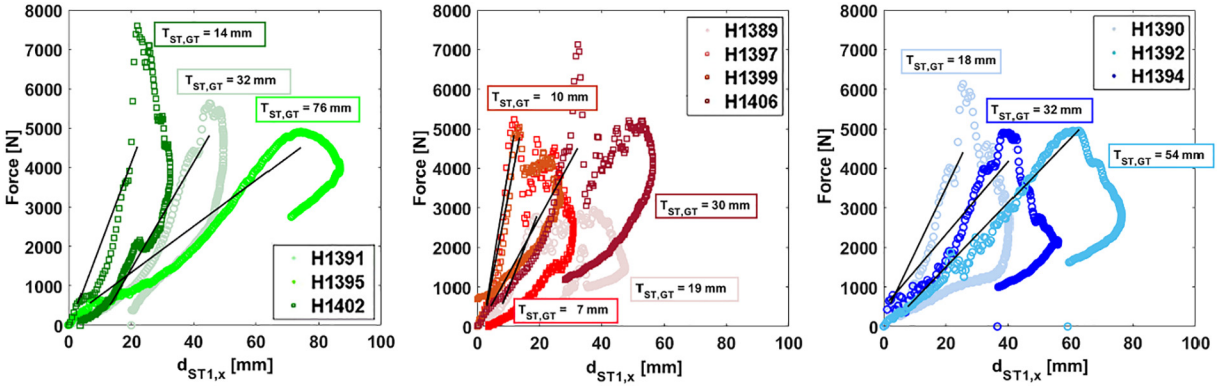

Fig. 6. Force over deflection in x-direction of marker ST1 for non-fracture outcomes (left), femoral fractures (middle), and pelvic fractures (right). The black lines show the spring characteristic for each specimen that was derived for model 1.

specimen and all but one [37] used rigid impact masses dropped onto the greater trochanter covered with a generic foam soft tissue surrogates. In comparison, our improved boundary conditions and subject-specific impact modelling resulted in the full spectrum of typical injuries that are related to falls with impact to the greater trochanter. The combination of fracture and non-fractures further allows for the validation of tools to predict fractures under conditions that are close to reality but still controlled.

We found that models with input information that was based on less severe impact conditions predicted lower impact forces than we found in our study. sDOF models by Robinovitch et al. [33], based on data which was used to create a relationship between the effective pelvic stiffness and the thickness of soft tissue over the greater trochanter, resulted in highly correlated predicted peak forces. However, force magnitudes were statistically significantly lower when compared to forces predicted by our model, resulting in predicted forces that would not suggest fracture in any specimen. This indicates that, if load predictions based on sDOF models are to be compared to femoral strength estimates, these sDOF models require input parameters that are dependent on trochanteric soft tissue thickness and impact velocity. Other models that were based on impact from low height resulted in very low peak force correlations with respect to our model and an underestimation of peak forces. The effective pelvic stiffness derived from our impacts was about 5 times larger than the stiffness derived from impacts from no height or very low height [32,33]. Compared to impacts from increased height onto a protective foam pad, the effective pelvic stiffness values calculated in the present study are about two times higher. Therefore, predicting impact force by using effective pelvic stiffness derived from low load levels can lead to systematic errors. A more complex model that considers the non-linearity of the force-deflection characteristic, as well as the complex energy balance in the system [67] could allow for a model that is predictive of sideways fall impact forces for impacts from low height and from standing. This is also highlighted by the ratio between torque impulse and angular momentum (Fig. 4), which showed that thinner trochanteric soft tissue thickness is associated with a smaller part of the initial angular momentum being transferred to the torque impulse, when comparing to bigger subjects. This is contradictory to system damping, which was found to be higher for subjects with thicker trochanteric soft tissue thickness in studies that simulated impacts with volunteers from low height.

The mechanical risk ratio that we calculated based on the estimated impact force and total hip aBMD was superior in terms of separating femur fractures from non-fracture outcomes. Peak forces predicted by model 2 were chosen because only the experimental peak forces of specimens that do not fracture reflect the force that acts onto the human body as a result of a simulated fall. Peak forces measured in specimens that fractured are determined by the strength of the failing structure. Therefore, the measured impact force underestimates the force that would have acted on the specimen had it not fractured. Since we used the experimental results to derive k_{m2} the accuracy of predictions for independent fall simulations is unclear. As expected, the sDOF models that used k_{m2} generally predict higher impact forces than the experimentally measured impact forces, except for one specimen. This highlights the importance of considering the patient-specific force that is applied to the human body as a result of a fall and the strength of the femur when attempting to estimate the potential for a particular fall resulting in a fracture. Subject-specific sDOF impact models should consider subject-specific effective body masses, subject-specific impact velocities based on body height [68], and subject-specific effective

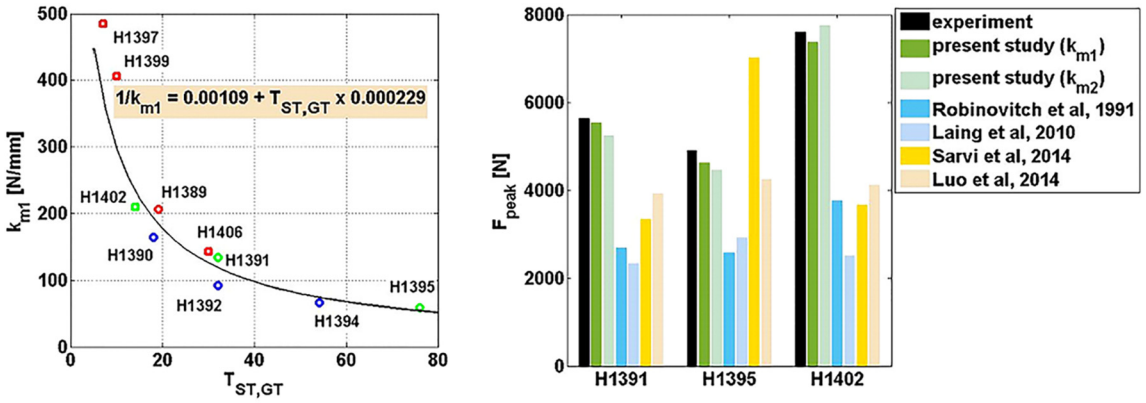

Fig. 7. sDOF models: (left) Calculated effective pelvic stiffness over soft tissue thickness. A linear fit was done for the effective pelvic compliance $1/k_{m1}$ as a function of $T_{ST,GT}$ (R^2 = 0.94); (right) calculated peak forces for non-fracture outcomes with comparison to implemented sDOF models from literature [31–33,52].

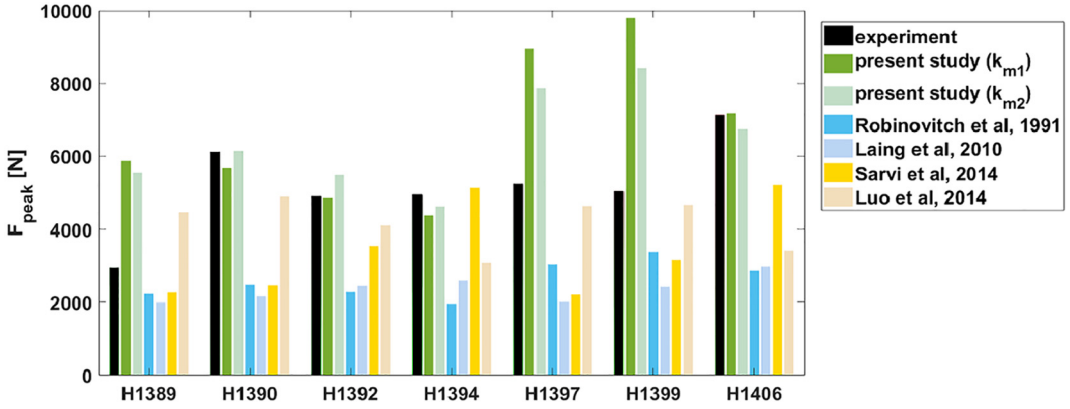

Fig. 8. Comparison of all measured peak forces with peak forces predicted by sDOF models for the current study and implemented models from literature [31–33,52].

pelvic stiffness values based on trochanteric soft tissue thickness and impact velocity. Femoral strength could be estimated based on femur aBMD or image-based finite element models [23,69,70]. In real life falls, other factors can influence the severity of an impact. Differences in reaction to imbalance, reaction time, and overall ability to "break a fall" will also play an important role for fracture risk assessment. These factors are not captured by the MRR and should be included based on other patient-specific information. The calculated MRR also did not separate pelvis fractures from non-fractures reliably. This suggests that aBMD might be a site-specific predictor of strength and other strength predictors are necessary to predict sideways fall-related pelvis fractures.

A limitation of our study is that a surrogate system was used, which only approximates the human body under impact and is not equivalent to a volunteer impacting onto a hard surface. More specifically, we neglected the influence of muscle activation and subject-specific tissue properties, the effect of the upper body, and considered overly rigid lower limbs. The strengths of the system are that impacts were controlled and subject-specific with reproducible alignment and impact velocity. The alignment of the pelvis and the femur with respect to the ground are especially important parameters to control in order to make falls comparable. Moreover, the tested body shape and soft tissue characteristics were controlled and known. This reduced bias when investigating parameters related to soft tissue shape and bones. A severe fall with the knee and the iliac crest impacting well after peak force was reached were modelled. The impact velocity (3.1 m/s) was close to the mean impact velocity that was reported for fall experiments with young volunteers (3.0 m/s) [71]. Furthermore, the increased effective pelvic stiffness is supported logically. To build up an impact force of *e.g.* 5000 N in a stiff male pelvis based on Robinovitch et al. (k = 50 N/mm), a deformation of 100 mm would be necessary. This is not feasible considering the amount of soft tissue over both greater trochanters, which would only amount to about 30 mm (2 × 15 mm). Pelvic deformations were recorded to be small (< 5 mm) in specimens that did not fracture the pelvis and typical femur deformation before fracture are low (< 4 mm) [17,72]. Consequently, the stiffness of the pelvic region needs to be much higher when loaded to high forces. Another limitation is that only one impact alignment and greater trochanter impact velocity was tested in this study to allow for better control and interpretation of the overall system and clearer conclusions to be drawn on the influence of soft tissue shape on the impact kinetics. In real life falls, patients might have a predisposition to fall more often or impact with higher or lower impact velocities. They might also have a preferred direction towards which they will try to guide the fall. These factors could not be considered in this study. The strengths of the system are the controlled conditions and that the hip could be loaded up to injurious force levels to investigate the impact kinetics at velocities that represent a severe fall, which is not ethical, even with young volunteers, due to the risk of injury.

5. Conclusion

This study provides direct evidence of the influence of various subject anthropometrics on the force experienced during sideways fall impact. The simulated impact showed subject-specific differences in

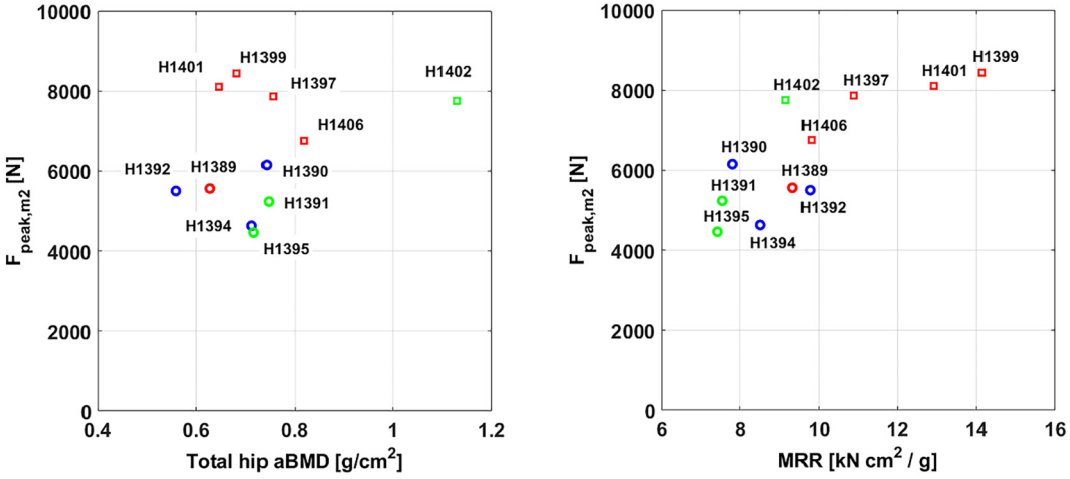

Fig. 9. (left) Predicted peak force *versus* total hip aBMD; (right) Predicted peak force *versus* mechanical risk ratio (MRR). Female specimens are marked with circles, male specimens with squares. The colours indicate impacts that resulted in a femur fracture (red), pelvis fracture (blue), or no fracture (green). (For interpretation of the references to colour in this figure legend, the reader is referred to the web version of this article.)

impact kinetics and resulted in clinically relevant femur fractures, pelvic fractures, and non-fractures. The described impact model provides an extension to impact models based on low height impact with volunteers and will provide valuable input to predict subject-specific impact forces at conditions that are representative of a fall from standing. The mechanical hip fracture risk assessment based on impact force and femur BMD was superior in separating femur fracture and non-fractures compared to femur aBMD alone. This result clearly points the way forward for improved screening for hip fracture risk.

Supplementary data to this article can be found online at https://doi.org/10.1016/j.bone.2019.05.004.

Conflict of interest

The authors have no conflict of interest related to this work.

Acknowledgement

Canada Diagnostics, Vancouver for their help with CT scanning specimens. This project was funded by the ETH Foundation (grant nr. ETH1514-1) the Swiss National Science Foundation (grant nr. 205320_16933) and UBC internal funds.

References

[1] W. Ekstrom, G. Nemeth, E. Samnegard, N. Dalen, J. Tidermark, Quality of life after a subtrochanteric fracture: a prospective cohort study on 87 elderly patients, Injury 40 (4) (2009) 371–376.
[2] S. Haleem, L. Lutchman, R. Mayahi, J.E. Grice, M.J. Parker, Mortality following hip fracture: trends and geographical variations over the last 40 years, Injury-International Journal of the Care of the Injured 39 (10) (2008) 1157–1163.
[3] E. Osnes, C. Lofthus, H. Meyer, J. Falch, L. Nordsletten, I. Cappelen, I.S. Kristiansen, Consequences of hip fracture on activities of daily life and residential needs, Osteoporos. Int. 15 (7) (2004) 567–574.
[4] E. Hernlund, A. Svedbom, M. Ivergard, J. Compston, C. Cooper, J. Stenmark, E.V. McCloskey, B. Jonsson, J.A. Kanis, Osteoporosis in the European Union: medical management, epidemiology and economic burden, Arch. Osteoporos. 8 (1–2) (2013).
[5] J. Parkkari, P. Kannus, M. Palvanen, A. Natri, J. Vainio, H. Aho, I. Vuori, M. Järvinen, Majority of hip fractures occur as a result of a fall and impact on the greater trochanter of the femur: a prospective controlled hip fracture study with 206 consecutive patients, Calcif. Tissue Int. 65 (1999) 183–187.
[6] J. Parkkari, P. Kannus, M. Palvanen, A. Natri, J. Vainio, H. Aho, I. Vuori, M. Jarvinen, Majority of hip fractures occur as a result of a fall and impact on the greater trochanter of the femur: a prospective controlled hip fracture study with 206 consecutive patients, Calcif. Tissue Int. 65 (3) (1999) 183–187.
[7] K. Sanders, K. Lim, A. Stuart, A. Macleod, D. Scott, G. Nicholson, L. Busija, Diversity in fall characteristics hampers effective prevention: the precipitants, the environment, the fall and the injury, Osteoporos. Int. 28 (10) (2017) 3005–3015.
[8] W.C. Hayes, E.R. Myers, S.N. Robinovitch, A. VandenKroonenberg, A.C. Courtney, T.A. McMahon, Etiology and prevention of age-related hip fractures, Bone 18 (1) (1996) S77–S86.
[9] N.M. Nachreiner, M.J. Findorff, J.F. Wyman, T.C. McCarthy, Circumstances and consequences of falls in community-dwelling older women, Journal of Womens Health 16 (10) (2007) 1437–1446.
[10] M.C. Nevitt, S.R. Cummings, S. Kidd, D. Black, Risk-factors for recurrent non-syncopal falls - a prospective-study, Jama-Journal of the American Medical Association 261 (18) (1989) 2663–2668.
[11] M.J. Bolland, A.T. Siu, B.H. Mason, A.M. Horne, R.W. Ames, A.B. Grey, G.D. Gamble, I.R. Reid, Evaluation of the FRAX and Garvan fracture risk calculators in older women, J. Bone Miner. Res. 26 (2) (2011) 420–427.
[12] J.A. Kanis, D. Hans, C. Cooper, S. Baim, J.P. Bilezikian, N. Binkley, J.A. Cauley, J.E. Compston, B. Dawson-Hughes, G.E.-H. Fuleihan, Interpretation and use of FRAX in clinical practice, Osteoporos. Int. 22 (9) (2011) 2395.
[13] S. Schuit, M. Van der Klift, A. Weel, C. De Laet, H. Burger, E. Seeman, A. Hofman, A. Uitterlinden, J. Van Leeuwen, H. Pols, Fracture incidence and association with bone mineral density in elderly men and women: the Rotterdam study, Bone 34 (1) (2004) 195–202.
[14] K.L. Stone, D.G. Seeley, L.Y. Lui, J.A. Cauley, K. Ensrud, W. Browner, M.C. Nevitt, S.R. Cummings, R. Osteoporotic Fractures, BMD at multiple sites and risk of fracture of multiple types: long-term results from the study of osteoporotic fractures, J. Bone Miner. Res. 18 (11) (2003) 1947–1954.
[15] S.A. Wainwright, L.M. Marshall, K.E. Ensrud, J.A. Cauley, D.M. Black, T.A. Hillier, M.C. Hochberg, M.T. Vogt, E.S. Orwoll, S.o.O.F.R. Group, Hip fracture in women without osteoporosis, The Journal of Clinical Endocrinology & Metabolism 90 (5) (2005) 2787–2793.
[16] E. Dall'Ara, B. Luisier, R. Schmidt, F. Kainberger, P. Zysset, D. Pahr, A nonlinear QCT-based finite element model validation study for the human femur tested in two configurations in vitro, Bone 52 (1) (2013) 27–38.
[17] D. Dragomir-Daescu, J. Op Den Buijs, S. McEligot, Y. Dai, R.C. Entwistle, C. Salas, L.J. Melton 3rd, K.E. Bennet, S. Khosla, S. Amin, Robust QCT/FEA models of proximal femur stiffness and fracture load during a sideways fall on the hip, Ann. Biomed. Eng. 39 (2) (2011) 742–755.
[18] K.K. Nishiyama, S. Gilchrist, P. Guy, P. Cripton, S.K. Boyd, Proximal femur bone strength estimated by a computationally fast finite element analysis in a sideways fall configuration, J. Biomech. 46 (7) (2013) 1231–1236.
[19] P. Varga, J. Schwiedrzik, P.K. Zysset, L. Fliri-Hofmann, D. Widmer, B. Gueorguiev, M. Blauth, M. Windolf, Nonlinear quasi-static finite element simulations predict in vitro strength of human proximal femora assessed in a dynamic sideways fall setup, J. Mech. Behav. Biomed. Mater. 57 (2016) 116–127.
[20] S. Amin, D.L. Kopperdhal, L.J. Melton 3rd, S.J. Achenbach, T.M. Therneau, B.L. Riggs, T.M. Keaveny, S. Khosla, Association of hip strength estimates by finite-element analysis with fractures in women and men, J. Bone Miner. Res. 26 (7) (2011) 1593–1600.
[21] J.H. Keyak, S. Sigurdsson, G. Karlsdottir, D. Oskarsdottir, A. Sigmarsdottir, S. Zhao, J. Kornak, T.B. Harris, G. Sigurdsson, B.Y. Jonsson, K. Siggeirsdottir, G. Eiriksdottir, V. Gudnason, T.F. Lang, Male-female differences in the association between incident hip fracture and proximal femoral strength: a finite element analysis study, Bone 48 (6) (2011) 1239–1245.
[22] J.H. Keyak, S. Sigurdsson, G.S. Karlsdottir, D. Oskarsdottir, A. Sigmarsdottir, J. Kornak, T.B. Harris, G. Sigurdsson, B.Y. Jonsson, K. Siggeirsdottir, G. Eiriksdottir, V. Gudnason, T.F. Lang, Effect of finite element model loading condition on fracture risk assessment in men and women: the AGES-Reykjavik study, Bone 57 (1) (2013) 18–29.
[23] D.L. Kopperdahl, T. Aspelund, P.F. Hoffmann, S. Sigurdsson, K. Siggeirsdottir, T.B. Harris, V. Gudnason, T.M. Keaveny, Assessment of incident spine and hip fractures in women and men using finite element analysis of CT scans, J. Bone Miner. Res. 29 (3) (2014) 570–580.
[24] T.F. Lang, S. Sigurdsson, G. Karlsdottir, D. Oskarsdottir, A. Sigmarsdottir, J. Chengshi, J. Kornak, T.B. Harris, G. Sigurdsson, B.Y. Jonsson, K. Siggeirsdottir, G. Eiriksdottir, V. Gudnason, J.H. Keyak, Age-related loss of proximal femoral strength in elderly men and women: the age gene/environment susceptibility study - Reykjavik, Bone 50 (3) (2012) 743–748.
[25] M. Nasiri, Y. Luo, Study of sex differences in the association between hip fracture risk and body parameters by DXA-based biomechanical modeling, Bone 90 (2016) 90–98.
[26] E.S. Orwoll, L.M. Marshall, C.M. Nielson, S.R. Cummings, J. Lapidus, J.A. Cauley, K. Ensrud, N. Lane, P.R. Hoffmann, D.L. Kopperdahl, T.M. Keaveny, G. Osteoporotic Fractures in Men Study, Finite element analysis of the proximal femur and hip fracture risk in older men, J. Bone Miner. Res. 24 (3) (2009) 475–483.
[27] A.L. Adams, H. Fischer, D.L. Kopperdahl, D.C. Lee, D.M. Black, M.L. Bouxsein, S. Fatemi, S. Khosla, E.S. Orwoll, E.S. Siris, Osteoporosis and hip fracture risk from routine computed tomography scans: the fracture, osteoporosis, and CT utilization study (FOCUS), J. Bone Miner. Res. 33 (7) (2018) 1291–1301.
[28] K.K. Nishiyama, M. Ito, A. Harada, S.K. Boyd, Classification of women with and without hip fracture based on quantitative computed tomography and finite element analysis, Osteoporos. Int. 25 (2) (2014) 619–626.
[29] C. Falcinelli, E. Schileo, L. Balistreri, F. Baruffaldi, B. Bordini, M. Viceconti, U. Albisinni, F. Ceccarelli, L. Milandri, A. Toni, F. Taddei, Multiple loading conditions analysis can improve the association between finite element bone strength estimates and proximal femur fractures: a preliminary study in elderly women, Bone 67 (2014) 71–80.
[30] M. Qasim, G. Farinella, J. Zhang, X. Li, L. Yang, R. Eastell, M. Viceconti, Patient-specific finite element estimated femur strength as a predictor of the risk of hip fracture: the effect of methodological determinants, Osteoporos. Int. 27 (9) (2016) 2815–2822.
[31] Y. Luo, M. Nasiri Sarvi, P. Sun, W.D. Leslie, J. Ouyang, Prediction of impact force in sideways fall by image-based subject-specific dynamics model, International Biomechanics 1 (1) (2014) 1–14.
[32] A.C. Laing, S.N. Robinovitch, Characterizing the effective stiffness of the pelvis during sideways falls on the hip, J. Biomech. 43 (10) (2010) 1898–1904.
[33] S.N. Robinovitch, W.C. Hayes, T.A. Mcmahon, Prediction of femoral impact forces in falls on the hip, Journal of Biomechanical Engineering-Transactions of the Asme 113 (4) (1991) 366–374.
[34] M.N. Sarvi, Y. Luo, Sideways fall-induced impact force and its effect on hip fracture risk: a review, Osteoporos. Int. 28 (10) (2017) 2759–2780.
[35] M.N. Sarvi, Y. Luo, A two-level subject-specific biomechanical model for improving prediction of hip fracture risk, Clin. Biomech. 30 (8) (2015) 881–887.
[36] A.J. Vandenkroonenberg, W.C. Hayes, T.A. McMahon, Dynamic-models for sideways falls from standing height, Journal of Biomechanical Engineering-Transactions of the Asme 117 (3) (1995) 309–318.
[37] S. Gilchrist, K.K. Nishiyama, P. de Bakker, P. Guy, S.K. Boyd, T. Oxland, P.A. Cripton, Proximal femur elastic behaviour is the same in impact and constant displacement rate fall simulation, J. Biomech. 47 (15) (2014) 3744–3749.
[38] D.P. Beason, G.J. Dakin, R.R. Lopez, J.E. Alonso, F.A. Bandak, A.W. Eberhardt, Bone mineral density correlates with fracture load in experimental side impacts of the pelvis, J. Biomech. 36 (2) (2003) 219–227.
[39] H. Guillemot, C. Got, B. Besnault, F. Lavaste, S. Robin, J.Y. Le Coz, J. Lassau, Pelvic behavior in side collisions: Static and dynamic tests on isolated pelvic bones, Proceedings of the 16th International Technical Conference of the Enhanced Safety of Vehicles, Windsor, ON, Canada, 1998, pp. 1412–1424.
[40] B.S. Etheridge, D.P. Beason, R.R. Lopez, J.E. Alonso, G. McGwin, A.W. Eberhardt, Effects of trochanteric soft tissues and bone density on fracture of the female pelvis in experimental side impacts, Ann. Biomed. Eng. 33 (2) (2005) 248–254.

[41] I.C. Levine, The Effects of Body Composition and Body Configuration on Impact Dynamics during Lateral Falls: Insights from In-Vivo, In-Vitro, and in-Silico Approaches, UWSpace, 2017.
[42] I. Fleps, M. Vuille, A. Melnyk, S.J. Ferguson, P. Guy, B. Helgason, P.A. Cripton, A novel sideways fall simulator to study hip fractures ex vivo, PLoS One 13 (7) (2018) e0201096.
[43] K. Comley, N.A. Fleck, The high strain rate response of adipose tissue, Iutam Symposium on Mechanical Properties of Cellular Materials, vol. 12, 2009, pp. 27–33.
[44] J.H. Mcelhaney, Dynamic response of bone and muscle tissue, J. Appl. Physiol. 21 (4) (1966) 1231–1236.
[45] B. Song, W. Chen, Y. Ge, T. Weerasoorlya, Dynamic and quasi-static compressive response of porcine muscle, J. Biomech. 40 (13) (2007) 2999–3005.
[46] J.B. Lauritzen, V. Askegaard, Protection against hip fractures by energy absorption, Dan. Med. Bull. 39 (1) (1992) 91–93.
[47] B. Lafleur, Factors Influencing Measures of Trochanteric Soft Tissue Thickness, University of Waterloo, 2016.
[48] B. Khoo, K. Brown, C. Cann, K. Zhu, S. Henzell, V. Low, S. Gustafsson, R. Price, R. Prince, Comparison of QCT-derived and DXA-derived areal bone mineral density and T scores, Osteoporos. Int. 20 (9) (2009) 1539–1545.
[49] P.J. Pickhardt, G. Bodeen, A. Brett, J.K. Brown, N. Binkley, Comparison of femoral neck BMD evaluation obtained using lunar DXA and QCT with asynchronous calibration from CT colonography, J. Clin. Densitom. 18 (1) (2015) 5–12.
[50] Y. Abdel-Aziz, H. Karara, M. Hauck, Direct linear transformation from comparator coordinates into object space coordinates in close-range photogrammetry, Photogramm. Eng. Remote Sens. 81 (2) (2015) 103–107.
[51] I.C. Levine, S. Bhan, A.C. Laing, The effects of body mass index and sex on impact force and effective pelvic stiffness during simulated lateral falls, Clin. Biomech. 28 (9–10) (2013) 1026–1033.
[52] M.N. Sarvi, Y. Luo, P. Sun, J. Ouyang, Experimental validation of subject-specific dynamics model for predicting impact force in sideways fall, J. Biomed. Sci. Eng. 07 (07) (2014) 405–418.
[53] X.G. Cheng, G. Lowet, S. Boonen, P.H.F. Nicholson, P. Brys, J. Nijs, J. Dequeker, Assessment of the strength of proximal femur in vitro: relationship to femoral bone mineral density and femoral geometry, Bone 20 (3) (1997) 213–218.
[54] A. Rezaei, D. Dragomir-Daescu, Femoral strength changes faster with age than BMD in both women and men: a biomechanical study, J. Bone Miner. Res. 30 (12) (2015) 2200–2206.
[55] D. Dragomir-Daescu, T.L. Rossman, A. Rezaei, K.D. Carlson, D.F. Kallmes, J.A. Skinner, S. Khosla, S. Amin, Factors associated with proximal femur fracture determined in a large cadaveric cohort, Bone 116 (2018) 196–202.
[56] W.C. Hayes, S.J. Piazza, P.K. Zysset, Biomechanics of fracture risk prediction of the hip and spine by quantitative computed-tomography, Radiol. Clin. N. Am. 29 (1) (1991) 1–18.
[57] J.N. Morris, J.A. Heady, P.A.B. Raffle, C.G. Roberts, J.W. Parks, Coronary heart-disease and physical activity of work, Lancet 265 (Nov21) (1953) 1053–1057.
[58] J.L. Kelsey, M.M. Prill, T.H. Keegan, C.P. Quesenberry Jr., S. Sidney, Risk factors for pelvis fracture in older persons, Am. J. Epidemiol. 162 (9) (2005) 879–886.
[59] M.L. Bouxsein, P. Szulc, F. Munoz, E. Thrall, E. Sornay-Rendu, P.D. Delmas, Contribution of trochanteric soft tissues to fall force estimates, the factor of risk, and prediction of hip fracture risk, J. Bone Miner. Res. 22 (6) (2007) 825–831.
[60] H.E. Meyer, A. Tverdal, J.A. Falch, Body height, body mass index, and fatal hip fractures: 16 years' follow-up of 674,000 Norwegian women and men, Epidemiology (1995) 299–305.
[61] T. Tang, P.A. Cripton, P. Guy, H.A. McKay, R. Wang, Clinical hip fracture is accompanied by compression induced failure in the superior cortex of the femoral neck, Bone 108 (2018) 121–131.
[62] E.M. Evans, The treatment of trochanteric fractures of the femur, J. Bone Joint Surg. 31 (2) (1949) 190–203 British.
[63] H. Pervez, M.J. Parker, G.A. Pryor, L. Lutchman, N. Chirodian, Classification of trochanteric fracture of the proximal femur: a study of the reliability of current systems, Injury 33 (8) (2002) 713–715.
[64] Femur, J. Orthop. Trauma 32 (2018) S33–S44.
[65] S.N. Robinovitch, S.L. Evans, J. Minns, A.C. Laing, P. Kannus, P.A. Cripton, S. Derler, S.J. Birge, D. Plant, I.D. Cameron, D.P. Kiel, J. Howland, K. Khan, J.B. Lauritzen, Hip protectors: recommendations for biomechanical testing-an international consensus statement (part I), Osteoporos. Int. 20 (12) (2009) 1977–1988.
[66] S.N. Robinovitch, T.A. McMahon, W.C. Hayes, Force attenuation in trochanteric soft tissues during impact from a fall, J. Orthop. Res. 13 (6) (1995) 956–962.
[67] I. Fleps, W.S. Enns-Bray, P. Guy, S.J. Ferguson, P.A. Cripton, B. Helgason, On the internal reaction forces, energy absorption, and fracture in the hip during simulated sideways fall impact, PloS one 13 (8) (2018) e0200952.
[68] A.J. van den Kroonenberg, W.C. Hayes, T.A. McMahon, Dynamic models for sideways falls from standing height, Transactions of the ASME. Journal of Biomechanical Engineering 117 (3) (1995).
[69] L. Grassi, S.P. Väänänen, M. Ristinmaa, J.S. Jurvelin, H. Isaksson, Prediction of femoral strength using 3D finite element models reconstructed from DXA images: validation against experiments, Biomech. Model. Mechanobiol. 16 (3) (2017) 989–1000.
[70] J.H. Keyak, S.A. Rossi, Prediction of femoral fracture load using finite element models: an examination of stress- and strain-based failure theories, J. Biomech. 33 (2) (2000) 209–214.
[71] F. Feldman, S.N. Robinovitch, Reducing hip fracture risk during sideways falls: evidence in young adults of the protective effects of impact to the hands and stepping, J. Biomech. 40 (12) (2007) 2612–2618.
[72] O. Ariza, S. Gilchrist, R.P. Widmer, P. Guy, S.J. Ferguson, P.A. Cripton, B. Helgason, Comparison of explicit finite element and mechanical simulation of the proximal femur during dynamic drop-tower testing, J. Biomech. 48 (2) (2015) 224–232.